Chapter 8

Isostasy

For a long time, isostasy has played a distinguished role in geodesy: Hayford used Pratt's model when, in 1911, he derived an ellipsoid which was adopted in 1924 as the International Ellipsoid, and Heiskanen applied Airy's model for computing the corresponding International Gravity Formula (1930). Isostatic gravity reduction always has been considered one of the best gravity reductions for geodetic purposes, but its computation was cumbersome before the advent of electronic computers.

Three effects contributed to the fact that, after 1960, isostatic reduction was somewhat relegated to the background: the theory of Molodensky, restricting itself purposely to the earth's surface, the advent of artificial satellites with their spectacular geodetic achievements, and also the relatively great computational work involved.

Still, isostasy was never completely forgotten: isostatic reduction was found to be compatible with Molodensky's theory, isostatic anomalies proved to be smoother than free-air anomalies and much less "systematic" than Bouguer anomalies, which made them ideally suited for interpolation and least-squares collocation. This was already clearly recognized in the sixties (cf. Heiskanen and Moritz, 1967).

Recently it was found that isostatic reduction applied to astronomically observed deflections of the vertical essentially facilitated the computation of the geoid in Alpine areas by least-squares collocation (cf. Sünkel et al., 1987). This and many other facts reconfirmed the importance of isostasy to geodesy.

The principle of isostatic compensation and its importance for a study of the crust has also always been recognized by geophysicists, although there was (and is) considerable controversy which isostatic model is applicable and to what extent. From this point of view, all isostatic models are only oversimplified approximations to reality. At any rate, most books on the physics of the earth, such as (Jeffreys, 1976), (Stacey, 1977), or (Turcotte and Schubert, 1982) treat isostasy under the heading "geodesy and gravity".

This chapter consists of three sections. First, the classical isostatic models of Pratt–Hayford, Airy–Heiskanen, and Vening Meinesz are briefly presented. Then the behavior of the free-air gravity anomalies (large but random), Bouguer anomalies (large and smooth but systematic) and isostatic anomalies (small, smooth and random) is explained on the basis of a simple two-layer dipole model. Finally, the recent theories of inverse problems for isostasy are treated, which nowadays enjoy considerable popularity in the geophysical community since none of the classical models is completely satisfactory from the geophysical point of view.

8.1 Classical Isostatic Models

From geodetic measurements performed around 1850 in India, J.H. Pratt in 1854 and 1859, and G.B. Airy in 1855 realized that the visible topographic masses of the Himalayan massif must somehow be compensated by mass deficiencies below sea level. According to Pratt, the mountains have risen from the underground somewhat like a fermenting dough. According to Airy, the mountains are floating on a fluid lava of higher density, so that the higher the mountain, the deeper it sinks; this behavior is rather similar to that of an iceberg floating in the ocean. In the next two subsections, we shall be following (Heiskanen and Moritz, 1967), using a plane approximation to the earth's surface or rather to the geoid.

8.1.1 The Model of Pratt–Hayford

This model of compensation was outlined by Pratt and put into a mathematical form by J.F. Hayford, who used it systematically for geodetic purposes.

The principle is illustrated by Fig. 8.1. Underneath the level of compensation there is uniform density. Above, the mass of each column of the same cross section is equal. Let D be the depth of the level of compensation, reckoned from sea level, and let ρ_0 be the density of a column of height D. Then the density ρ of a column of height $D + h$ (h representing the height of the topography) satisfies the equation

$$(D+h)\rho = D\rho_0 \quad , \tag{8–1}$$

which expresses the condition of equal mass. It may be assumed that

$$\rho_0 = 2.67\,\mathrm{g/cm^3} \quad . \tag{8–2}$$

According to (8–1), the actual density ρ is slightly smaller than this normal value ρ_0. Consequently, there is a density deficiency which, according to (8–1), is given by

$$\Delta\rho = \rho_0 - \rho = \frac{h}{D+h}\rho_0 \quad . \tag{8–3}$$

In the oceans the condition of equal mass is expressed as

$$(D-h')\rho + h'\rho_w = D\rho_0 \quad , \tag{8–4}$$

where

$$\rho_w = 1.027\,\mathrm{g/cm^3} \tag{8–5}$$

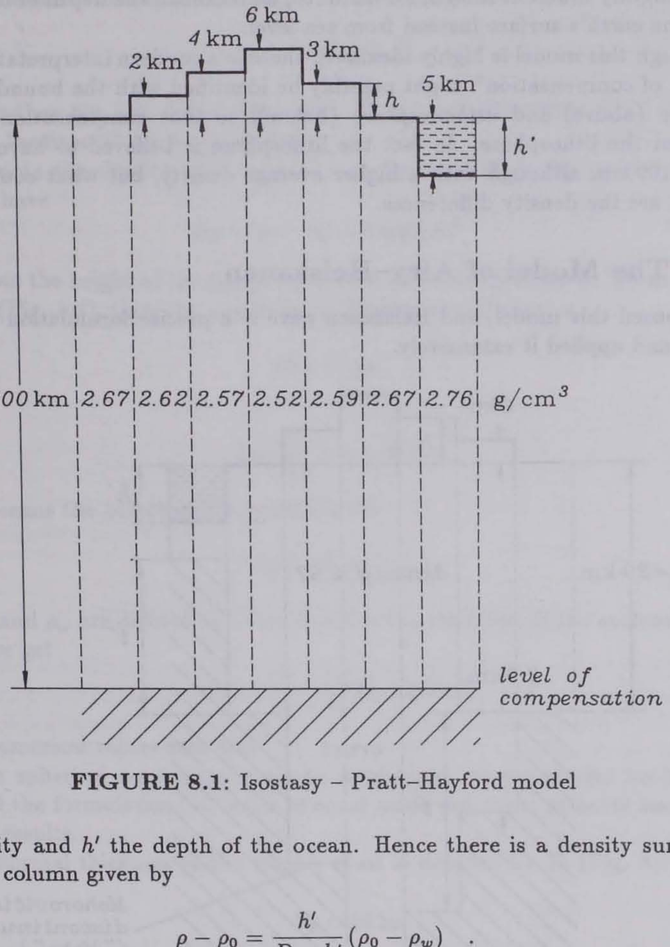

FIGURE 8.1: Isostasy – Pratt–Hayford model

is the density and h' the depth of the ocean. Hence there is a density surplus in a suboceanic column given by

$$\rho - \rho_0 = \frac{h'}{D - h'} (\rho_0 - \rho_w) \quad . \tag{8–6}$$

As a matter of fact, this model of compensation can be only approximately fulfilled in nature. Values of the depth of compensation around

$$D = 100 \, \text{km} \tag{8–7}$$

are assumed.

For a spherical earth, the columns will converge slightly towards its center, and other refinements may be introduced. We may postulate either equality of mass or equality of pressure; each postulate leads to somewhat different spherical refinements. It may be mentioned that for computational reasons Hayford used still another, slightly different model; for instance, he reckoned the depth of compensation D from the earth's surface instead from sea level.

Although this model is highly idealized, there is a modern interpretation in which the "level of compensation" might possibly be identified with the boundary between *lithosphere* (above) and *asthenosphere* (below), so that compensation takes place throughout the lithosphere. In fact the lithosphere is believed to have a thickness of about 100 km, although with a higher average density, but what counts for compensation are the density differences.

8.1.2 The Model of Airy–Heiskanen

Airy proposed this model, and Heiskanen gave it a precise formulation for geodetic purposes and applied it extensively.

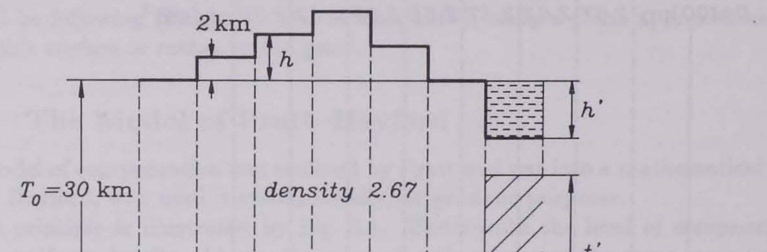

FIGURE 8.2: Isostasy – Airy–Heiskanen model

Figure 8.2 illustrates the principle. The mountains, of constant density (say)

$$\rho_0 = 2.67\,\mathrm{g/cm^3} \quad , \tag{8–8}$$

float on a denser underlayer of constant density (say)

$$\rho_1 = 3.27\,\mathrm{g/cm^3} \quad . \tag{8–9}$$

The higher they are, the deeper they sink. Thus, *root formations* exist under mountains, and "antiroots" under the oceans.

We denote the density difference $\rho_1 - \rho_0$ by $\Delta\rho$. With the assumed numerical values we have

$$\Delta\rho = \rho_1 - \rho_0 = 0.6\,\mathrm{g/cm^3} \quad . \tag{8–10}$$

If we denote the height of the topography by h and the thickness of the corresponding root by t (Fig. 8.2), then the condition of floating equilibrium is

$$t\Delta\rho = h\rho_0 \quad , \tag{8–11}$$

so that

$$t = \frac{\rho_0}{\Delta\rho}\,h = 4.45\,h \quad . \tag{8–12}$$

For the oceans the corresponding condition is

$$t'\Delta\rho = h'(\rho_0 - \rho_w) \quad , \tag{8–13}$$

where h' and ρ_w are defined as above and t' is the thickness of the antiroot (Fig. 8.2), so that we get

$$t' = \frac{\rho_0 - \rho_w}{\rho_1 - \rho_0}\,h' = 2.74\,h' \tag{8–14}$$

for the numerical values assumed.

Again spherical corrections must be applied to these formulas for higher accuracy, and the formulations in terms of equal mass and equal pressure lead to slightly different results.

The normal thickness of the earth's crust is denoted by T_0 (Fig. 8.2). Values of around

$$T_0 = 30\,\mathrm{km} \tag{8–15}$$

are assumed. The crustal thickness under mountains is then

$$T_0 + h + t \quad , \tag{8–16}$$

and under the oceans it is

$$T_0 - h' - t' \quad . \tag{8–17}$$

What we have called above "denser underlayer" is, of course, the *mantle* separated by the crust by the *Mohorovičić discontinuity*, or briefly, the *Moho*. The mantle evidently is not liquid, but over very long time spans, even apparently "solid" materials behave in a plastic way, not unlike a very viscous fluid.

8.1.3 Regional Compensation According to Vening Meinesz

Both systems just discussed are highly idealized in that they assume the compensation to be strictly *local*; that is, they assume that compensation takes place along vertical columns. This presupposes free vertical mobility of the masses to a degree that is obviously unrealistic in this strict form.

For this reason, Vening Meinesz (1931, 1940, 1941) modified the Airy floating theory, introducing regional instead of local compensation. The principal difference between these two kinds of compensation is illustrated in Fig. 8.3. In Vening Meinesz'

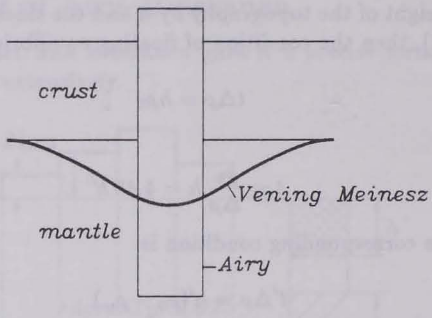

FIGURE 8.3: Local and regional compensation

theory, the topography is regarded as a load on an unbroken but yielding elastic crust.

To understand the situation, consider a point load P on an infinite plane elastic plate (representing the crust) which floats on a viscous underlayer of higher density (representing the mantle, see above); see Fig. 8.4. Since the topography is counted

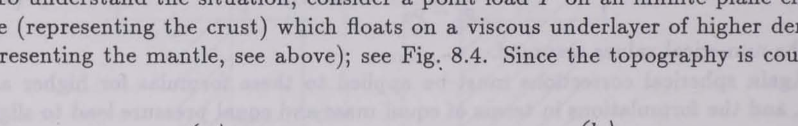

FIGURE 8.4: Bending (direct effect, (a)) and thickening (indirect effect, (b)) of an elastic plate

above sea level, we must fill the upper hollow in Fig. 8.4, (a), by crustal material of density ρ_0 which causes, as an additional load, a further bending (indirect effect)

(Fig. 8.4, (b)). Since the upper boundary is to remain horizontal, the total effect is a thickening of the plate. If m_P denotes the mass of the point load, then its weight, or the force it exerts on the plate, obviously is $m_P g$, g being gravity as usual.

Fig. 8.5 shows the lower boundary of this plate. This boundary surface is obtained

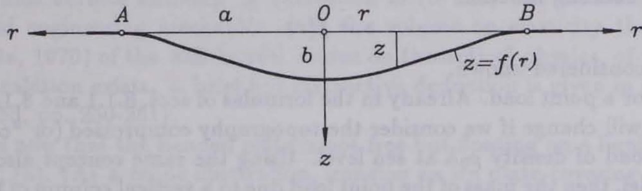

FIGURE 8.5: The bending curve

by rotating the bending curve around the z-axis; we obviously presuppose isotropy. We further assume the curve to be nonzero only in the region $r < a$, $a = AO = OB$, and to be tangent to the coordinate axes at the end points A and B. (In modern terminology, $f(r)$ is a "function of compact support", cf. sec. 7.5.)

The equilibrium condition obviously is

$$(\rho_1 - \rho_0) \iint_S f(r) dS = 1 \quad , \tag{8–18}$$

if the mass m_P of the point load P is considered 1 (1 kg or 1 ton, say), S being the circle of radius a around O. This equation expresses the fact that the point load of mass 1 (right–hand side) is balanced by the hydrostatic uplift caused by the density difference $\rho_1 - \rho_0$ (left–hand side).

The bending curve is given by Hertz' theory of the bending of an elastic plate, as we shall see below. What we need now are only the principal functional values (Table 8.1). The constants l (Vening Meinesz' "degree of regionality") and b must be

TABLE 8.1: The bending curve after Hertz and Vening Meinesz

r	$f(r)$
0	b
l	$0.646\,b$
$2\,l$	$0.258\,b$
$3\,l$	$0.066\,b$
$3.887\,l$	0.000

selected appropriately; obviously

$$a = 3.887\,l \quad . \tag{8–19}$$

To be sure, $f(r)$ is not exactly zero for $r > a$, but periodic, representing small circular waves with constantly decreasing amplitudes.

Vening Meinesz, however, put $f(r) = 0$ outside $3.887\,l$ (more precisely, already outside $2.905\,l$ in order to enforce (8–18) for a *finite* circle around O) and approximated $f(r)$ piecewise by polynomials (nowadays we would use a spline approximation). At any rate, the bending function

$$z = f(r) \tag{8–20}$$

is now to be considered known.

So much for a point load. Already in the formulas of secs. 8.1.1 and 8.1.2 it is clear that nothing will change if we consider the topography compressed (or "condensed") as a surface load of density $\rho_0 h$ at sea level. Using the same concept also in Vening Meinesz' model, then the mass of the point load due to a vertical column of topography of cross section dS becomes

$$dm = \rho_0 h dS \quad .$$

Since $z = f(r)$ corresponds to a unit mass load, the bending due to the column under consideration is

$$z\,dm = \rho_0 h dS\, f(r) \quad ,$$

and the total bending Z due to the entire topography will be

$$Z(x, y) = \iint z\,dm = \rho_0 \iint h(x', y') f(r) dx' dy' \quad , \tag{8–21}$$

the integral being formally extended over the whole plane. Note that z has dimension: length per unit mass. Since

$$r = \sqrt{(x - x')^2 + (y - y')^2} \quad ,$$

the above formula represents Z as a *linear convolution* of the functions h and f.

Finally we note that

$$T = T_0 + Z \tag{8–22}$$

will be the depth of the Moho below sea level, T_0 being the "normal thickness of the earth's crust" of Airy–Heiskanen, as given, for instance, by (8–15).

Physical background. For those readers who have some knowledge of elastostatics or are otherwise interested in the physical basis of Vening Meinesz' theory, we shall outline the background, which is of considerable mathematical interest, also in view of the fact that, in Chapter 7, we have used the bipotential equation in a quite different context; cf. eq. (7–109).

It is well known that a plane elastic plate satisfies the "plate equation"

$$D \Delta^2 z = p \quad . \tag{8–23a}$$

Here

$$\Delta^2 = \left(\frac{\partial^2}{\partial x^2} + \frac{\partial^2}{\partial y^2} \right)^2 = \frac{\partial^4}{\partial x^4} + 2 \frac{\partial^4}{\partial x^2 y^2} + \frac{\partial^4}{\partial y^4}$$

represents the *biharmonic operator* in two dimensions (the upper boundary of the unbended plate is the xy-plane); cf. eq. (7–11) for three dimensions. The quantity z expresses the vertical displacement of the plate by bending; for a unit mass load, it is identical to (8–20) above. The "plate stiffness" D is a constant depending on the elastic properties of the plate and of its thickness, and p represents the load force on a unit surface element. A derivation of (8–23a) can be found in any text on advanced engineering mechanics or in the volume on elasticity theory (Landau and Lifschitz, 1970) of the well-known course on theoretical physics, of which also an English translation exists. A brief but instructive deduction is given in (Courant and Hilbert, 1953, pp. 250-251).

Suppose now that the bended plate is not free but floating on a liquid underlayer, cf. Fig. 8.4, (a). (As a crude illustration, imagine an ice plate covering a lake, which is bent by the weight of a man standing on it.) Then the hydrostatic uplift causes a force

$$g\rho_1 z$$

on a unit surface element, which acts opposite to the load p and must be subtracted from it. Thus (8–23a) is to be replaced by

$$D\Delta^2 z = p - g\rho_1 z \quad . \tag{8–23b}$$

This case was first considered by Hertz (1884) and is given a lengthy elementary treatment by Föppl (1922, pp. 103–119), to whom Vening Meinesz refers. Eq. (8–23b) is also used, without derivation, in (Jeffreys, 1976, p. 270).

Eq. (8–23b) represents to the "direct effect", cf. Fig. 8.4, (a). To get a horizontal upper surface, we must fill up the upper hollow. This produces a force

$$g\rho_0 z$$

per unit area, which acts in the same direction as p and thus must be added to the right-hand side of (8–23b), with the result

$$D\Delta^2 z = p - g(\rho_1 - \rho_0)z \quad . \tag{8–23c}$$

Thus the "indirect effect" is taken into account by simply replacing ρ_1 in (8–23b) by the density contrast (8–10)! This case was not considered by Hertz and may have first been treated by Vening Meinesz. For a somewhat different physical model leading to the same result (cf. Turcotte and Schubert, 1982, pp. 121-122).

Consider now a point load of mass 1 concentrated at the origin (in modern terminology, we would call it a "delta function load"). Outside the origin, p is zero, so that (8–23c) becomes

$$D\Delta^2 z = -g(\rho_1 - \rho_0)z$$

except for $x = y = 0$, or

$$\Delta^2 z + l^{-4} z = 0 \quad , \tag{8–24a}$$

where

$$l = \sqrt[4]{\frac{D}{g(\rho_1 - \rho_0)}}$$

has the dimension of a length and is nothing else than Vening Meinesz' "degree of regionality" mentioned above; he considers values of l from 10 to 60 km.

Solution of Hertz' equation. Because of rotational symmetry, it is best to transform (8–24a) to polar coordinates. Since

$$z = f(r)$$

is a function of

$$r = \sqrt{x^2 + y^2}$$

only, we get

$$\frac{\partial z}{\partial x} = \frac{dz}{dr}\frac{\partial r}{\partial x} = \frac{dz}{dr}\frac{x}{r}\,, \quad \text{etc.,}$$

so that we can express the Laplace operator

$$\Delta = \frac{\partial^2}{\partial x^2} + \frac{\partial^2}{\partial y^2} = \frac{d^2}{dr^2} + \frac{1}{r}\frac{d}{dr}$$

for functions of r only. Thus, with $l^{-1} = k$, eq. (8–24a) becomes

$$\left[\left(\frac{d^2}{dr^2} + \frac{1}{r}\frac{d}{dr}\right)\left(\frac{d^2}{dr^2} + \frac{1}{r}\frac{d}{dr}\right) + k^4\right] z = 0 \tag{8–24b}$$

or, since with $i^2 = -1$,

$$a^4 + b^4 = (a^2 + i\,b^2)(a^2 - i\,b^2) \quad ,$$

further

$$\left(\frac{d^2}{dr^2} + \frac{1}{r}\frac{d}{dr} + i\,k^2\right)\left(\frac{d^2}{dr^2} + \frac{1}{r}\frac{d}{dr} - i\,k^2\right) z = 0 \quad . \tag{8–24c}$$

Now

$$\frac{d^2u}{dx^2} + \frac{1}{x}\frac{du}{dx} + u = 0 \tag{8–25a}$$

is the well-known *Bessel equation* (of zero order), whose solutions are, e.g., Bessel's function

$$u = J_0(x)$$

and Hankel's functions

$$u = H_0^{(1)}(x) \quad \text{and} \quad u = H_0^{(2)}(x) \quad ;$$

cf., e.g., (Courant and Hilbert, 1953, pp. 467–471). Solutions of the equation

$$\frac{d^2u}{dx^2} + \frac{1}{x}\frac{du}{dx} \pm i\,k^2 u = 0 \tag{8–25b}$$

will consequently be the functions

$$J_0(kx\sqrt{\pm i}) \;, \quad H_0^{(1)}(kx\sqrt{\pm i}) \quad \text{and} \quad H_0^{(2)}(kx\sqrt{\pm i}) \quad , \tag{8–26a}$$

and these functions will obviously also solve (8–24c).

The functions, or linear combinations of them, are known as *Kelvin functions*; splitting into a real and an imaginary part we have, e.g.,

$$\begin{aligned} \operatorname{ber} x + i \operatorname{bei} x &= J_0(x\sqrt{-i}) \quad , \\ \ker x + i \operatorname{kei} x &= \frac{1}{2}\pi i\, H_0^{(1)}(x\sqrt{-i}) \quad . \end{aligned} \tag{8–26b}$$

This all sounds very complicated, but we simply need a solution which is finite, with horizontal tangent, at the origin and vanishes at infinity. Looking at standard tables (Janke and Emde, 1945) and (Abramowitz and Stegun, 1965), we find without difficulty the required functions: (Janke and Emde, 1945) shows in the graph on p. 250 and the table on p. 252 that the real part of $H_0^{(1)}(x\sqrt{i})$ does the job, and so likewise do (Abramowitz and Stegun, 1965) in the graph on p. 382 and the table on p. 431: here $\operatorname{kei}(x)$ is the required solution. Both functions are identical, apart from a constant factor. If we norm them to have $f(0) = 1$, we get from both tables the values shown in Table 8.2 (multiply the values in Janke–Emde by 2, and the values in

TABLE 8.2: Enlarged and corrected version of Table 8.1, with $l = b = 1$

x	$f(x)$
0	1.0000
0.5	0.8551
1.0	0.6302
1.5	0.4219
2.0	0.2577
2.5	0.1409
3.0	0.0651
3.5	0.0204
3.915	0.0000

Abramowitz–Stegun by $-4/\pi$). No further knowledge of Bessel functions is required: just use the table as if it were a table of sines or cosines! (Cf. also Turcotte, 1979, p. 66.)

The difference between the values of Tables 8.1 and 8.2 is not surprising if we note that Hertz (1884), for functions which are not easy to calculate after all, had only limited computational facilities, and that Vening Meinesz simply took Hertz' values.

To return to our physical model, we finally remark that Hertz (1884, p. 452) gives, in our notations, m_P denoting the mass of the point load:

$$b = f(0) = \frac{m_P}{8\rho_1 l^2} \quad .$$

If we consider a unit point mass load ($m_P = 1$) and replace ρ_1 by the density contrast $\rho_1 - \rho_0$ as we have seen above, we get

$$b = \frac{1}{8(\rho_1 - \rho_0)l^2} \quad .$$

This represents a relation between l, the density contrast, and the maximum depth of bending under a unit point load; it is identical to Vening Meinesz' (1940) eq. (1B). This value obviously must be in agreement with (8–18).

A simplified case. As we have seen, the two-dimensional equation (8–24a), in the case of rotational symmetry, can only be solved by somewhat unusual functions. Suppressing the y-coordinate, however, we get an extremely simple solution which gives an excellent qualitative (though not quantitative) picture of the problem and thus will facilitate our understanding (Turcotte and Schubert, 1982, pp. 125–126).

Disregarding the dependence on y, we have $\Delta^4 z = d^4 z/dx^4$, so that (8–24a) reduces to

$$\frac{d^4 z}{dx^4} + l^{-4} z = 0 \quad .$$

This is a linear ordinary differential equation with constant coefficients, for which the general solution is readily found by standard methods. It is

$$\begin{aligned} z &= e^{x/\alpha}\left(c_1 \cos\frac{x}{\alpha} + c_2 \sin\frac{x}{\alpha}\right) + \\ &\quad + e^{-x/\alpha}\left(c_3 \cos\frac{x}{\alpha} + c_4 \sin\frac{x}{\alpha}\right) \quad ; \end{aligned}$$

the constants c_i are to be determined by the boundary conditions and $\alpha = l\sqrt{2}$.

The requirement that the deformation z vanishes at infinity ($x \to \infty$) immediately eliminates, for positive x, the terms multiplied by $e^{x/\alpha}$, so that $c_1 = c_2 = 0$. Furthermore, the condition of a horizontal tangent at the origin $x = 0$ gives $c_3 = c_4$, so that our final solution simply is

$$z = b e^{-x/\alpha}\left(\cos\frac{x}{\alpha} + \sin\frac{x}{\alpha}\right) \qquad (x \geq 0) \tag{8–27}$$

as the equation of our "one-dimensional bending curve"; we have put $c_3 = c_4 = b$ in agreement with our former notations.

In fact, for small x we may expand this function into a Taylor series:

$$z = b\left(1 - \frac{x^2}{\alpha^2} + \frac{2x^3}{3\alpha^3} \cdots\right) \quad ,$$

which is immediately seen to give $dz/dx = 0$ for $x = 0$; the term linear in x is missing only if $c_3 = c_4$! To have symmetry with respect to $x = 0$ (corresponding to the origin $r = 0$ in Fig. 8.5), we must replace x by $|x|$, which produces a step discontinuity in $d^3 z/dx^3$ and hence the required delta-like singularity in $d^4 z/dx^4$ at $x = 0$, corresponding to a point load; cf. sec. 3.3.2.

To repeat, this extremely simple solution is not the equation of the actual bending curve (8–20) but gives an excellent qualitative picture. This can be seen by drawing the graph of (8–27), with x replaced by $-x$ for negative values of x: a central depression surrounded by very small waves of decreasing amplitude.

8.1.4 Attraction of the Compensating Masses

As a preparatory step for computing isostatic reductions, to be discussed in sec. 8.1.5, we need the attraction of the compensating masses. For simplicity we consider the problem in the usual local plane approximation, replacing the geoid by its tangential plane. The spherical approximation will be used later (sec. 8.2).

We shall assume a basic definition concerning our three-dimensional local Cartesian coordinate system (Fig. 8.6): The xy-plane represents sea level, the z-axis points

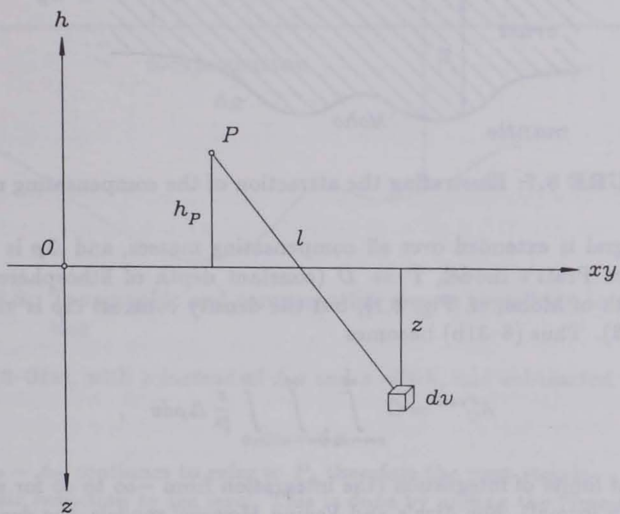

FIGURE 8.6: The basic coordinate systems xyz and xyh

vertically *downwards*, whereas the h-axis points vertically *upwards*, so that, for an arbitrary point,

$$z = -h \quad . \tag{8–28}$$

Keeping this definition in mind, the distance l between the computation point P and the volume element dv becomes

$$l^2 = (z + h_P)^2 + (x - x_P)^2 + (y - y_P)^2 \quad . \tag{8–29}$$

The potential V_C of the compensating masses thus is

$$V_C = G \iiint \frac{\Delta\rho}{l}\, dv \tag{8–30}$$

and their attraction (positive downward)

$$A_C = -\frac{\partial V_C}{\partial h_P} = G \iiint \frac{h_P + z}{l^3}\, \Delta\rho dv \tag{8–31a}$$

with $\partial l^{-1}/\partial h_P$ by (8–29). For a point at sea level ($h_P = 0$) this reduces to

$$A_C = G \iiint \frac{z}{l^3}\, \Delta\rho dv \quad . \tag{8–31b}$$

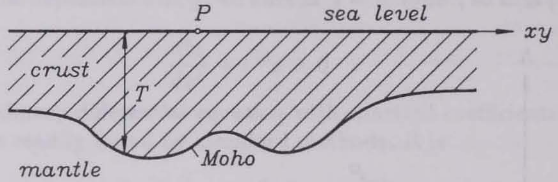

FIGURE 8.7: Illustrating the attraction of the compensating masses

The integral is extended over all compensating masses, and $\Delta\rho$ is their density contrast. For Pratt's model, $T \Rightarrow D$ (constant depth of lithosphere rather than variable depth of Moho, cf. Fig. 8.1), but the density contrast $\Delta\rho$ is variable, being given by (8–3). Thus (8–31b) becomes

$$A_C^{Pratt} = G \int\limits_{x=-\infty}^{\infty} \int\limits_{y=-\infty}^{\infty} \int\limits_{z=0}^{D} \frac{z}{l^3}\, \Delta\rho dv \quad , \tag{8–32a}$$

with constant limits of integration (the integration from $-\infty$ to ∞ for x and y is, of course, purely formal). For Airy's and Vening Meinesz' models, the density contrast $\Delta\rho = \rho_1 - \rho_0$ is constant ($0.6\,\mathrm{g/cm^3}$, say), but the Moho depth T is variable (Fig. 8.7), so that for these models,

$$A_C = G\Delta\rho \iint\limits_{-\infty}^{\infty} \int\limits_{z=T_0}^{T} \frac{z}{l^3}\, dv \quad . \tag{8–32b}$$

The integrals are to be evaluated by numerical integration, using standard methods (cf. Heiskanen and Moritz, 1967, pp. 117–118; Forsberg, 1984).

Very similar integrals hold, of course, for the attraction of the topography, as we shall see in what follows.

8.1.5 Remarks on Gravity Reduction

Gravity reduction may be summarized as follows (for more details cf. (Heiskanen and Moritz, 1967, pp. 130–151)):

1. *Removal of topography.* Gravity g_P is measured at a surface point P (Fig. 8.8). The attraction A_T of the topographic masses above sea level is computed by a similar

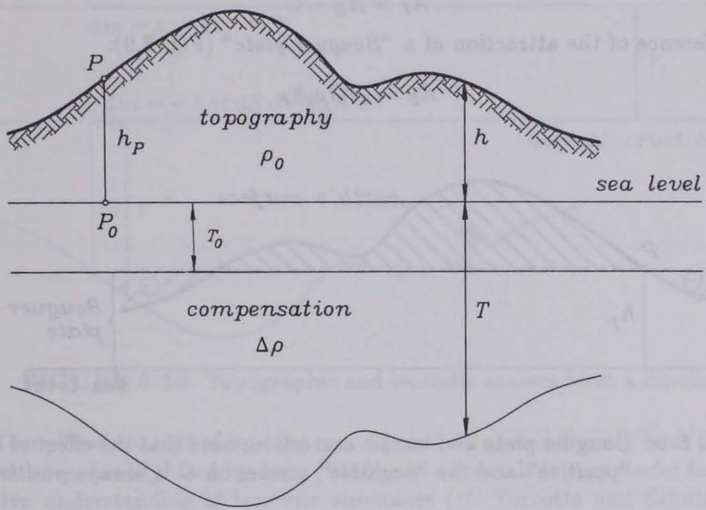

FIGURE 8.8: Topographic and compensating masses contribute to gravity reduction

formula as (8–31a), with ρ instead of $\Delta\rho$ and $z = -h$, and subtracted from g_P. The result is

$$g_P - A_T \quad . \tag{8–33}$$

However, $g_P - A_T$ continues to refer to P, therefore the next step is

2. *Free-air reduction to sea level.* This is done by adding the "free-air reduction"

$$F = -\frac{\partial\gamma}{\partial h} h_P \doteq 0.3086\, h_P \,\text{mgal} \quad , \tag{8–34}$$

with h_P in meters. (The *milligal*, abbreviated mgal, is the conventional unit for gravity differences: $1\text{mgal} = 10^{-5}\,\text{m}\,\text{s}^{-2}$.) The replacement of actual gravity g by normal gravity γ is only an approximation, and the numerical value given in (8–34) is conventional. The result is *Bouguer gravity*

$$g_B = g_P - A_T + F \quad . \tag{8–35}$$

Subtracting normal gravity γ we get the *Bouguer anomaly*

$$\Delta g_B = g_B - \gamma = g_P - A_T + F - \gamma \quad . \tag{8–36}$$

3. *Effect of isostatic compensation.* This effect A_C as expressed by (8–31b) is to be added to (8–36) to give the *isostatic anomaly*

$$\Delta g_I = \Delta g_B + A_C = g_P - A_T + A_C + F - \gamma \quad . \tag{8–37}$$

Bouguer plate and topographic correction. The attraction A_T is conventionally computed as

$$A_T = A_B - C \tag{8–38}$$

as the difference of the attraction of a *"Bouguer plate"* (Fig. 8.9):

$$A_B = 2\pi G \rho_0 h_P \tag{8–39}$$

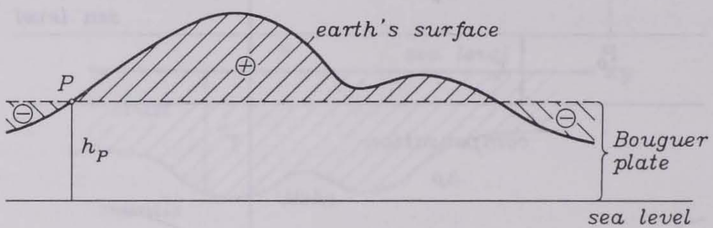

FIGURE 8.9: Bouguer plate and terrain correction; note that the effect of both the "positive" and the "negative" masses on C is always positive

and a *"topographic correction"*, or *"terrain correction"*, C which is usually quite small but *always positive.* For more details cf. (Heiskanen and Moritz, 1967, pp. 130–133); see also sec. 8.2.2 below. Isostatic and other reduced gravity anomalies may also be defined so as to refer to the topographic earth surface rather than to sea level. This is the modern conception related to Molodensky's theory, which is outside the scope of the present book (cf. Heiskanen and Moritz, 1967, secs. 8–2 and 8–11; Moritz, 1980, Part D).

8.2 Isostasy as a Dipole Field

In the case of local compensation, the isostatically compensating mass inside a vertical column is exactly equal to the topographic mass contained in the same column. This holds for both the Pratt and the Airy concept, by the very principle of local compensation. Fig. 8.10 illustrates the situation for the Airy–Heiskanen model. Approximately, the topography may be "condensed" as a surface layer on sea level S_0, whereas the compensation, with appropriate opposite sign, is thought to be concentrated as a surface layer on the surface S_T parallel to S_0 at constant depth T (T is our former T_0). Both surface elements dm for topography and $-dm$ for compensation thus form a dipole. This fact is also expressed by the difference $A_C - A_T$ in (8–37).